UNLV | UNIVERSITY LIBRARIES

2013

Transparent actuator made with few layer graphene electrode and dielectric elastomer, for variable focus lens

Taeseon Hwang
University of Nevada, Las Vegas

Hyeok-Yong Kwon
Sungkyunkwan University

Joon-Suk Oh
Sungkyunkwan University

Jung-Pyo Hong
Sungkyunkwan University

Seung-Chul Hong
Sungkyunkwan University
Follow this and additional works at: https://digitalscholarship.unlv.edu/me_fac_articles

Part of the Atomic, Molecular and Optical Physics Commons, Electrical and Computer Engineering
Commons, Mechanical Engineering Commons, and the Nanoscience and Nanotechnology Commons
See next page for additional authors

Repository Citation

Authors

Taeseon Hwang, Hyeok-Yong Kwon, Joon-Suk Oh, Jung-Pyo Hong, Seung-Chul Hong, Youngkwan Lee, Hyouk Ryeo Choi, Kwang J. Kim, Mainul Hossain Bhuiya, and Jae Do Nam

Transparent actuator made with few layer graphene electrode and dielectric elastomer, for variable focus lens

Taeseon Hwang, Hyeok-Yong Kwon, Joon-Suk Oh, Jung-Pyo Hong, Seung-Chul Hong, Youngkwan Lee, Hyouk Ryeol Choi, Kwang Jin Kim, Mainul Hossain Bhuiya, and Jae-Do Nam

CrossMark
click for updates

Transparent actuator made with few layer graphene electrode and dielectric elastomer, for variable focus lens

Taeseon Hwang,[1,2] Hyeok-Yong Kwon,[3] Joon-Suk Oh,[1] Jung-Pyo Hong,[1] Seung-Chul Hong,[1] Youngkwan Lee,[4] Hyouk Ryeol Choi,[3] Kwang Jin Kim,[2,3,a] Mainul Hossain Bhuiya,[2] and Jae-Do Nam[1,5,a]

[1]Department of Polymer Science and Engineering, Sungkyunkwan University, Suwon 440330, South Korea
[2]Active Materials and Processing Laboratory, Department of Mechanical Engineering, University of Nevada, Las Vegas, Nevada 89154-4027, USA
[3]Department of Mechanical Engineering, Sungkyunkwan University, Suwon 440330, South Korea
[4]Department of Chemical Engineering, Sungkyunkwan University, Suwon 440330, South Korea
[5]Department of Energy Science, Sungkyunkwan University, Suwon 440330, South Korea

A transparent dielectric elastomer actuator driven by few-layer-graphene (FLG) electrode was experimentally investigated. The electrodes were made of graphene, which was dispersed in N-methyl-pyrrolidone. The transparent actuator was fabricated from developed FLG electrodes. The FLG electrode with its sheet resistance of 0.45 kΩ/sq (80 nm thick) was implemented to mask silicone elastomer. The developed FLG-driven actuator exhibited an optical transparency of over 57% at a wavenumber of 600 nm and produced bending displacement performance ranging from 29 to 946 μm as functions of frequency and voltage. The focus variation was clearly demonstrated under actuation to study its application-feasibility in variable focus lens and various opto-electro-mechanical devices. © 2013 AIP Publishing LLC. [http://dx.doi.org/10.1063/1.4812982]

Variable-focus lenses have been extensively considered in a wide range of applications, such as cameras, projectors, mobile phones, and machine vision.[1,2] The focusing can be achieved by mechanical stress,[2,3] electrochemistry,[4] and electro-wetting.[5] Various authors have studied electroactive polymer (EAP) actuators as variable-focus lenses. For example, an ionic polymer-metal composite (IPMC) was used as a lens which gave an actuation of 0.413–0.608 mm,[6] and a cantilever-shape IPMC actuator exerted pressure on a liquid that was in contact with a transparent polydimethylsiloxane lens.[7] A carbon-polymer composite actuator has been used to drive a liquid-based variable-focal lens device.[8] In these EAP-based variable-focus lens systems, however, the actuator is typically used to tune the shape of a passive lens made of liquids. In contrast to the liquid tunable lenses, an all-solid-state and self-actuating polymer lens can very well to mimic the working principle of the human eye lens. Additionally, the solid-state lenses can better withstand fluctuations in temperature, pressure, and motion compared to liquid-based lenses, which offer a more robust approach to tunable optical systems.[9]

The lens effect is achieved when the optical paths of the light beams propagating through different parts of the medium are different. Thus, the lens can be formed either by varying the thickness of the material (as in conventional glass lenses) or by varying the refractive index across the light beam.[10] If the dielectric elastomer is flat, there is no focusing effect. When voltage is applied across the elastomer while the edges are fixed, the expansions of the elastomer along the lateral direction would result in a deformed surface

of the elastic elastomer which would eventually attain convex or concave shape. The origin of the actuation in this system is a mechanical pressure generated by the electrical potential across the dielectric material, known as Maxwell stress (see Fig. S1 in supplementary material[31])

$$P = \varepsilon_o \varepsilon_r E^2, \tag{1}$$

$$E = v/t, \tag{2}$$

where P is the Maxwell stress and ε_o and ε_r denote the permittivity of free space and the relative permittivity of the elastomer, respectively. E, V, and t represent the electric field, applied voltage, and thickness of the dielectric elastomer, respectively. Therefore, the key elements for the development of the variable-focus lens in the solid state are the transparency of the dielectric elastomer and electrode materials which would actuate and deform to generate various refractive indices. Indium tin oxide (ITO) is the most commonly used transparent electrode material in various display systems, such as organic light emitting diodes, touch screens, and liquid crystal displays. However, ITO is too brittle and stiff to be used in dielectric elastomer actuators (DEAs). Several alternative transparent electrodes have been investigated, including thin metal films,[11] carbon nanotube random meshes,[12] metal nano-wire random meshes,[13] and conducting polymers.[14] Poly(3,4-ethylenedioxythiophene) has been successfully deposited on the surfaces of silicone rubber elastomer to give a transparent solid-state actuator,[14] demonstrating its capability as a compliant electrode for changing the focal length of the incident beam. While substantial progress has been made in those transparent and compliant electrode systems, many issues still remain to be addressed in terms of performance, durability, lifetime, surface roughness, manufacturability, etc.

a)Authors to whom correspondence should be addressed. Electronic addresses: kwang.kim@unlv.edu and jdnam@skku.edu. Phone: +1 702 774 1419 (K. J. Kim). Phone: +82 31 290 7285 (J.-D. Nam).

103, 023106-1

Graphene is a single-atom-thick planar sheet of carbon atoms that are densely packed in a honeycomb crystal lattice. It has attracted much attention due to its ultrahigh mechanical strength,[15] electrical conductivity,[16] and optical transparency.[17] In this study, few-layer graphene (FLG), which is composed of a few graphene layers, has been considered as electrode material for flexible electrodes because it is transparent, bendable, strong adhesive, and electrically conductive. The transparencies for a single layer of graphene were reported to be 97.7% for the mechanically exfoliated graphene and 97.4% for chemical vapor deposited graphene.[18,19] The liquid-phase exfoliated graphene sheet has been reported to give a sheet resistance (Rs) of 5 KΩ/sq and a transmittance of 90%.[20] The graphene oxide (GO) has also been investigated for being used as a transparent electrode usually through the thermal reduction processes.[21] Although a significant number of defects remain after thermal reduction, the electrical resistance reduces as compared to that fabricated from the liquid exfoliated graphene dispersion.[22] The vacuum-filtered FLG film also gave a transparent conductive layer on a bendable plastic substrate with a strong cohesive van der Waals force between the FLG film and the substrate.[23]

In the present study, we prepared FLG dispersion by expanding the graphite with microwave radiation followed by physio-chemical exfoliation of the expanded graphite in *N*-methyl-pyrrolidone. The FLG dispersion is poured over the anodic aluminum oxide (AAO) membrane while a vacuum is applied underneath to develop the FLG film electrode. In this process, the FLG is oriented in the in-plane direction due to the vertical direction of the vacuum. When the FLG film attached AAO membrane was place on the water surface, the hydrophobic FLG film was easily separated from the hydrophilic AAO membrane. To fabricate the FLG-driven actuator, the FLG film on the water surface was carefully transferred onto the masked silicone substrate (hydrophobic) by scooping up the FLG film using the masked silicone substrate. The transfer process was driven by the difference in adhesive strength of the two surfaces between water-FLG film and FLG film-masked silicone substrate (see Fig. S2 in supplementary material).[24,25,31]

The morphology of the individual FLG was probed by a transmission electron microscopy (TEM) with a drop casting the dispersion onto a porous grid (mesh sizes of 200). Fig. 1(a) shows that the individual FLG is composed of a few layers of graphene and its edges tend to scroll and fold slightly. The Raman spectra were obtained with an RXN1 spectrometer using 633 nm (Ar$^+$ laser) excitation. Fig. 1(b) presents Raman spectra of the pristine graphite and FLG film. The G band at ~1580 cm^{-1} and 2D band at ~2700 cm^{-1} are clearly visible in the spectra of the graphite and FLG film. However, the D band at ~1350 cm^{-1} is only visible in the spectrum of the FLG film. The prominent G band of graphite at 1580 cm^{-1} corresponds to the first order scattering of the tangential stretching (E2g) mode. The weak D band at approximately 1350 cm^{-1} originates from the disordered structure at the graphite edges. The D band at 1350 cm^{-1} indicates the destruction of the graphite sp^2 structure by the ultrasonic process, resulting in the formation of sp^3 bonds in the carbon network.[26] The D band of the FLG film has higher intensity than that of graphite, seemingly because of the

number of defects in the FLG structure is increased by both exfoliation and sonication processes. The peak positions and relative intensities of the G band (~1580 cm^{-1}) and 2D band (~2700 cm^{-1}) of the two samples are similar. This suggests that the graphene obtained in our study is composed of a few layers of graphene.[27] Fig. 1(c) presents the scanning electron microscopy (SEM) image of the FLG film transferred onto the silicone substrate. The surface of the FLG film shows that many individual FLGs are uniformly stacked on the silicone substrate. In order to compare composition of specimens, X-ray photoelectron spectroscopy (XPS) was performed with a monochromatic Al Kα X-ray source. Fig. 1(d) shows the C1s narrow scans of the FLG film prepared in our experiment. The C1 (284.6 ± 0.2 eV) and C2 (285.7 ± 0.2 eV) peaks are attributed to carbon in the non-oxygenated sp^2 and sp^3 C-C bonds, respectively. The additional peaks of C3 (286.8.0 ± 0.2 eV) and C4 (288.2 ± 0.2 eV) are ascribed to carbon in the C–O and C=O bonds, respectively. These XPS results of the FLG film are similar to those obtained for graphite. In the case of oxidized graphene, or GO, the C1s XPS spectrum usually exhibits larger C–O and C=O peaks compared to graphite.[28] The XPS analysis suggests that our FLG film is not substantially oxidized. In addition, the Rs and transmittance of the FLG film (80 nm in thickness) were measured to be 0.45 kΩ/sq and 65% (at a wavenumber of 600 nm), respectively.

For the fabrication of the FLG-driven actuator, the FLG film floating on the water surface was carefully transferred onto the masked silicone substrate by scooping up the FLG film [Figs. 2(a) and 2(b)]. The FLG film transferred onto the masked silicone substrate was then dried at 150 °C for 24 h under vacuum to complete the bonding [Fig. 2(c)]. Subsequently, the mask was removed from the silicone substrate [Fig. 2(d)]. Similarly, the other side of the electrode was fabricated by repeating the same processes in Figs. 2(a) through 2(d) [Fig. 2(e)]. The resulting FLG-driven actuator (top and bottom FLG electrodes) is transparent, so we can see
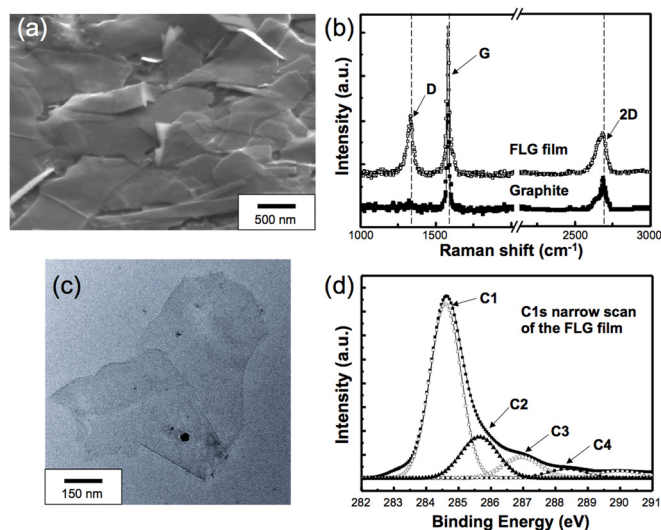

FIG. 1. The characterization of the individual FLG and the transferred FLG film: (a) TEM image of an individual FLG, (b) the Raman spectra (633 nm) of the pristine graphite and the FLG film, (c) SEM image of the transferred FLG film, and (d) XPS spectrum of the FLG film (C1s narrow scan).
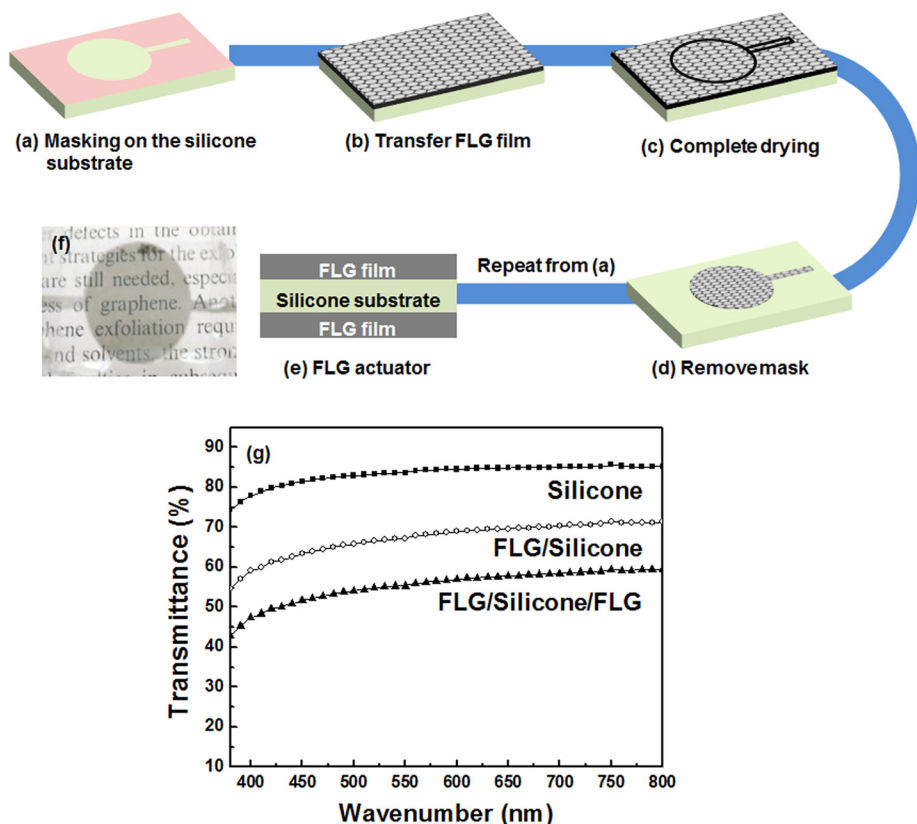
FIG. 2. Preparation of the FLG-driven actuator: (a) masking on the silicone substrate, (b) transfer FLG film via the transfer technique, (c) complete drying at 150 °C for 24 h under vacuum, (d) repeating the transfer to attach the FLG film to the opposite side of the silicone substrate and remove the mask, (e) side view of FLG-driven actuator, and (f) camera image of the FLG-driven actuator. (g) Transmittance of the silicone elastomer, FLG/silicone, and FLG/silicone/FLG in the visible light wavelength region.

the text underneath the FLG-driven actuator as shown in Fig. 2(f). A quantitative demonstration of the transmittance measurement in the visible range wavelength region (380–800 nm) is shown in Fig. 2(g). It compares the transmittance of three types of actuator: FLG/silicone, FLG/silicone/FLG, and pristine silicone elastomer (100 μm in thickness). The transmittance of the pristine silicone elastomer was found to be 84.5% at a wavenumber of 600 nm. When the FLG electrode was deposited on the silicone elastomer, transmittance decreased to 68.9%, which subsequently decreased to 57.0% for the FLG/silicone/FLG actuator.

The performance of the actuator as a function of the supply voltage was measured with a laser displacement sensor. The voltage supplied to the actuator ranged from 1 to 4 kV, and the frequency was varied from 1 to 5 Hz (sinusoidal and tangential waveforms). Fig. 3(a) shows the displacement (vertical position variation from flat surface) of the FLG-driven actuator (a thickness of 100 μm) as a function of time measured at various voltages. As the actuating voltage increases from 1 to 4 kV (at a fixed frequency of 1 Hz), the displacement of the FLG-driven actuator increases and the maximum displacement of the actuator reaches up to 946 μm. The maximum displacement is displayed as a function of applied voltage in Fig. 3(b). According to the actuation principles of the DEAs, the compression force varies directly as a function of applied voltage. Therefore, the displacement of the actuator increases with the voltage applied to the FLG-driven actuator.[29] In addition, Figs. 3(c) and 3(d) show the displacement of the FLG-driven actuator at various frequencies from 1 to 5 Hz (at a fixed voltage of 3.0 kV). The displacement slightly increases to 11 μm in the range of 1–2 Hz although the maximum displacement decreases from

916 μm at 2 Hz to 674 μm at 5 Hz. This is due to the molecular orientation or relaxation time decrease with the frequency increases.[14,30]

A digital single lens reflex (DSLR) camera was used for the measurement of focal length change. The angle of view and the aperture of the lens were 50 mm and F 8.0, respectively. Figs. 4(a) and 4(b) show the photographs of the FLG-driven actuator, comparing the stages with voltage "ON" and "OFF." When the voltage is "ON," the FLG actuator bends in the meniscus shape as can be clearly seen in Fig. 4(b). By attaching the FLG-driven actuator on the DSLR camera, images were captured through the FLG actuator in order to investigate the changes in the focal length. As seen in Fig. 4(c), the manuscript image can clearly be observed in the voltage "OFF" state. When the voltage turns "ON," as seen in Fig. 4(d), the manuscript image becomes out of focus and blurred due to the altered focal length triggered by the FLG-driven actuator, which deformed to meniscus shape result from the thickness of center is thinner than that of the boundary.[14] This result confirms that the focal length can be altered by varying the voltage input at FLG-driven actuator from the flat shape to the curved-lens shape. It suggests that this FLG-driven actuator has the potential to be used in opto-electro-mechanical applications, such as lenses, sensors, and touch screens. In addition, the lifetime and durability should be the important factor to apply opto-electro-mechanical devices. Therefore, the lifetime and durability would be further investigated in the future.

In summary, the FLG-driven actuator was successfully demonstrated by transferring the FLG film to the dielectric elastomer film using the transfer technique. We characterized the FLG film on a silicone substrate surface by Raman
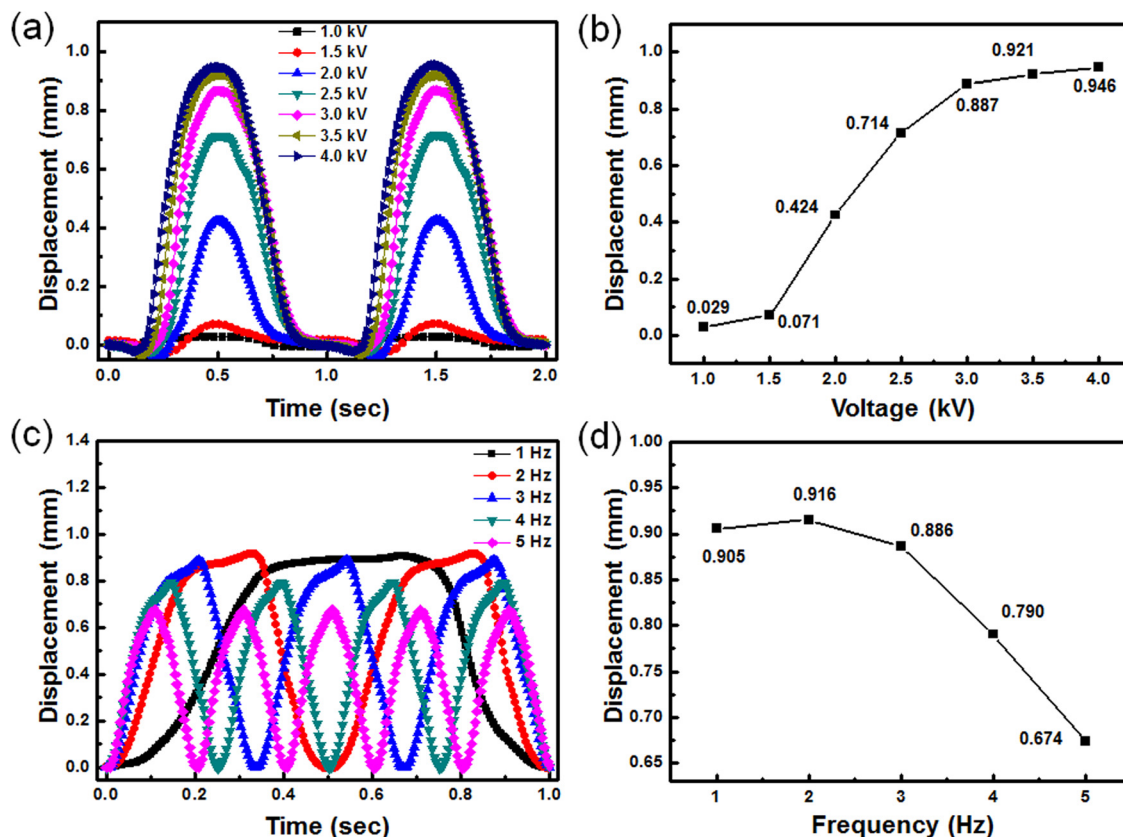
FIG. 3. Displacement of the FLG-driven actuator (a thickness of 100 μm) at various voltages at 1 Hz (a) and its maximum displacement (b). The displacement of the FLG-driven actuator (a thickness of 100 μm) at various frequencies at 3 kV (c) and its maximum displacement (d).

spectroscopy, SEM, TEM, and the XPS technique. The transmittance of the FLG-driven actuator film was investigated using UV-Vis spectroscopy. The displacement of the FLG-driven actuator at 100 μm in thickness was measured as a function of time with a laser displacement sensor as the voltage was varied from 1 to 4 kV at 1 Hz and as the frequency was varied from 1 to 5 Hz at 3 kV. We confirmed that the focal length could be changed by the developed FLG-driven actuator.
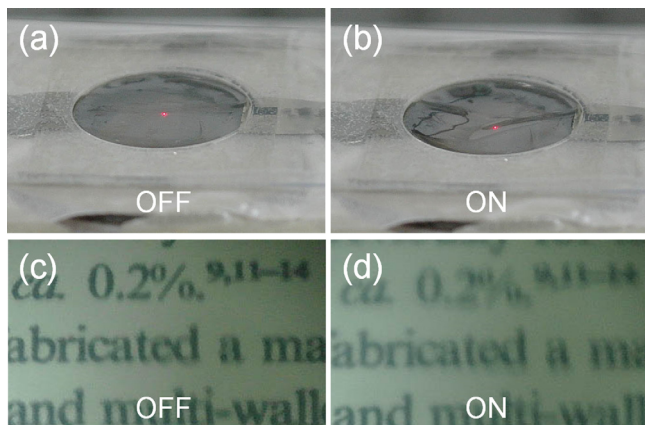
FIG. 4. Photographs of the FLG-driven actuator captured by the DSLR camera in the states of voltage "OFF" (a) and "ON" (b). The manuscript images through the FLG-driven actuator is compared in (c) and (d), each corresponding to the voltage "OFF" and "ON," respectively (applied voltage at 4 kV).

[1]X. Zeng and H. Jiang, Appl. Phys. Lett. **93**, 151101 (2008).
[2]H. Ren and S.-T. Wu, Appl. Phys. Lett. **86**, 211107 (2005).
[3]D. Y. Zhang, V. Lien, Y. Berdichevsky, J. Choi, and Y.-H. Lo, Appl. Phys. Lett. **82**, 3171 (2003).
[4]C. A. Lopez, C.-C. Lee, and A. H. Hirsa, Appl. Phys. Lett. **87**, 134102 (2005).
[5]C. Li and H. Jiang, Appl. Phys. Lett. **100**, 231105 (2012).
[6]H. K. Lee, N.-J. Choi, S. Jung, S. Lee, H. Jung, J. W. Ryu, and K.-H. Park, SPIE Rev. **6927**, 69271N (2008).
[7]A. Matteo and P. Maurizio, Smart Mater. Struct. **21**, 105030 (2012).
[8]S. W. Lee and S. S. Lee, Appl. Phys. Lett. **90**, 121129 (2007).
[9]G. Beadie, M. L. Sandrock, M. J. Wiggins, R. S. Lepkowicz, J. S. Shirk, M. Ponting, Y. Yang, T. Kazmierczak, A. Hiltner, and E. Baer, Opt. Express **16**, 11847 (2008).
[10]O. Pishnyak, S. Sato, and O. D. Lavrentovich, Appl. Opt. **45**, 4576 (2006).
[11]R. B. Pode, C. J. Lee, D. G. Moon, and J. I. Han, Appl. Phys. Lett. **84**, 4614 (2004).
[12]J. Li, L. Hu, L. Wang, Y. Zhou, G. Grüner, and T. J. Marks, Nano Lett. **6**, 2472 (2006).
[13]J. Y. Lee, S. T. Connor, Y. Cui, and P. Peumans, Nano Lett. **8**, 689 (2008).
[14]S. I. Son, D. Pugal, T. Hwang, H. R. Choi, J. C. Koo, Y. Lee, K. Kim, and J. D. Nam, Appl. Opt. **51**, 2987 (2012).
[15]V. P. Verma, S. Das, I. Lahiri, and W. Choi, Appl. Phys. Lett. **96**, 203108 (2010).

[16]Y. Wang, X. Chen, Y. Zhong, F. Zhu, and K. P. Loh, Appl. Phys. Lett. **95**, 063302 (2009).

[17]B. J. Kim, C. Lee, Y. Jung, K. H. Baik, M. A. Mastro, J. K. Hite, J. C. R. Eddy, and J. Kim, Appl. Phys. Lett. **99**, 143101 (2011).

[18]K. S. Kim, Y. Zhao, H. Jang, S. Y. Lee, J. M. Kim, K. S. Kim, J. H. Ahn, P. Kim, J.-Y. Choi, and B. H. Hong, Nature (London) **457**, 706 (2009).

[19]X. Li, W. Cai, J. An, S. Kim, J. Nah, D. Yang, R. Piner, A. Velamakanni, I. Jung, E. Tutuc, S. K. Banerjee, L. Colombo, and R. S. Ruoff, Science **324**, 1312 (2009).

[20]P. Blake, P. D. Brimicombe, R. R. Nair, T. J. Booth, D. Jiang, F. Schedin, L. A. Ponomarenko, S. V. Morozov, H. F. Gleeson, E. W. Hill, A. K. Geim, and K. S. Novoselov, Nano Lett. **8**, 1704 (2008).

[21]X. Wang, L. Zhi, and K. Mullen, Nano Lett. **8**, 323 (2008).

[22]S. De, P. J. King, M. Lotya, A. O'Neill, E. M. Doherty, Y. Hernandez, G. S. Duesberg, and J. N. Coleman, Small **6**, 458 (2010).

[23]T. Hwang, J. S. Oh, J. P. Hong, G.-Y. Nam, A. H. Bae, S. I. Son, G. H. Lee, H. K. Sung, Y. Lee, and J. D. Nam, Carbon **50**, 612 (2012).

[24]D. R. Hines, S. Mezhenny, M. Breban, E. D. Williams, V. W. Ballarotto, G. Esen, A. Southard, and M. S. Fuhrer, Appl. Phys. Lett. **86**, 163101 (2005).

[25]S. Wang, Y. Zhang, N. Abidi, and L. Cabrales, Langmuir **25**, 11078 (2009).

[26]K. N. Kudin, B. Ozbas, H. C. Schniepp, R. K. Prud'homme, I. A. Aksay, and R. Car, Nano Lett. **8**, 36 (2008).

[27]Q. Hao, S. M. Morton, B. Wang, Y. Zhao, L. Jensen, and T. J. Huang, Appl. Phys. Lett. **102**, 011102 (2013).

[28]Q. Feng, Q. Cao, M. Li, F. Liu, N. Tang, and Y. Du, Appl. Phys. Lett. **102**, 013111 (2013).

[29]R. Pelrine, R. Kornbluh, Q. Pei, and J. Joseph, Science **287**, 836 (2000).

[30]J. D. Nam, S. D. Hwang, H. R. Choi, J. H. Lee, K. J. Kim, and S. Heo, Smart Mater. Struct. **14**, 87 (2005).

[31]See supplementary material at http://dx.doi.org/10.1063/1.4812982 for detailed lens effect of the electroactive polymer and the experimental details.